



scattering (SAXS) experiments on beamline BM26B revealed that it is possible to switch from elongated, rod-like assemblies to small and discrete objects (Figures 68 and 69), by balancing attractive non-covalent forces within the hydrophobic core of the polymerising building blocks with electrostatic repulsive interactions on the hydrophilic rim.

Furthermore, the concentration dependent aggregation process of rod-like stacks could be studied as suggested by SAXS profiles: at 0.25 mM of discotic 1, rods of 23 nm in length and 6.2 nm in diameter are formed. At 0.5 mM the rod length is 27 nm and at 1 mM the length increases well above 75 nm. The order in the self-assembled objects and their growth mechanism were also characterised using circular dichroism, UV/Vis and $^1\text{H-NMR}$ spectroscopy. In line with our continuous efforts in elucidating the mechanisms of supramolecular polymerisations [2], we have focussed on correlating the morphological properties of the materials with the appropriate mechanistic details of the self-assembly pathways: cooperative growth of monomer 1 leads to very high molecular weight supramolecular polymers, whereas frustrated growth of discotic 2 and the resulting anticooperativity, results in the formation of small and discrete objects, without compromising their

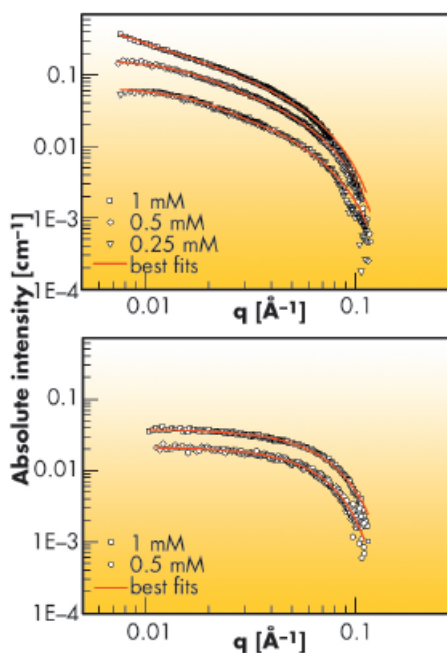


Fig. 69 SAXS profiles of the self-assembled discotics 1 (upper graph) and 2 (lower graph) at different concentrations.

thermodynamic stability. The latter are very promising building blocks for the development of supramolecular magnetic resonance imaging (MRI) contrast agents.

This is a unique example for directional self-assembly in water whereby the supramolecular polymer shape and size can be dictated by Coulombic interactions. In analogy to many systems found in nature, mechanistic details of the self-assembly process emphasise the importance of cooperativity as a key feature that dictates the physical properties of the supramolecular polymers.

References

- [1] L.C. Palmer, Y.S. Velichko, M. Olvera de la Cruz and S.I. Stupp, *Phil. Trans. R. Soc. A* 365, 1417-1433 (2007).
- [2] T.F.A. de Greef, M.M.J. Smulders, M. Wolfs, A.P.H.J. Schenning, R.P. Sijbesma and E.W. Meijer, *Chem. Rev.* 109 5687-5754 (2009).

Ultrafast X-ray solution scattering reveals different reaction pathways in the photolysis of $\text{Ru}_3(\text{CO})_{12}$ after ultraviolet and visible excitation

The triangular metal carbonyl cluster, $\text{Ru}_3(\text{CO})_{12}$, plays an important role in photocatalysis and photoenergy conversion and has served as the paradigm for the photochemistry of transition metal carbonyls. However, detailed mechanisms for the photochemical reactions are rarely available, mainly due to the lack of efficient methods to study them. Ultrafast X-ray solution scattering has been shown to give information that is generally difficult to extract from

ultrafast optical spectroscopy such as the time course of changes in bond lengths and angles, including those of short-lived intermediates, on a timescale of picoseconds to milliseconds [1]. Following this approach, our recent time-resolved X-ray solution scattering study on $\text{Ru}_3(\text{CO})_{12}$ in cyclohexane excited at 390 nm revealed a new intermediate, $\text{Ru}_3(\text{CO})_{10}$, that escaped detection in a previous spectroscopic study [2].

Principal publication and authors

- Q.Y. Kong (a), J.H. Lee (b), K.H. Kim (b), J.H. Kim (b), M. Wulff (c), H. Ihee (b) and M.H.J. Koch (d), *J. Am. Chem. Soc.* 132, 2600-2607 (2010).
(a) Synchrotron SOLEIL, GIF-sur-Yvette (France)
(b) Center for Time-Resolved Diffraction, Department of Chemistry, Graduate School of Nanoscience and Technology (WCU), KAIST, Daejeon (Republic of Korea)
(c) ESRF
(d) EMBL, Hamburg Outstation, EMBL c/o DESY, Hamburg (Germany)

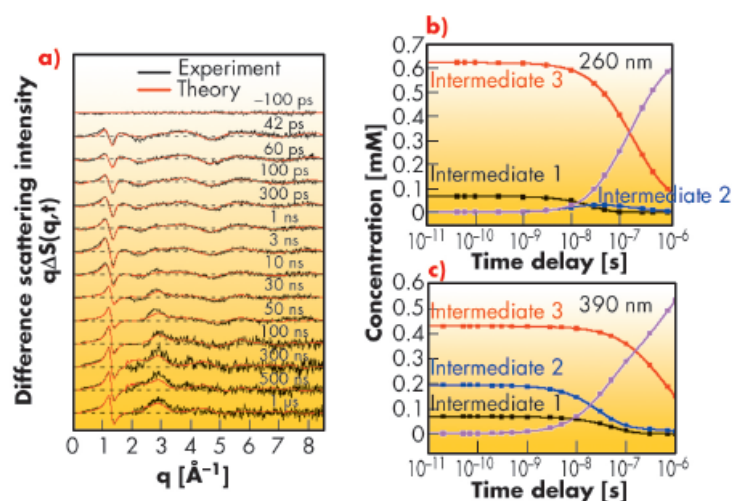


Fig. 70: a) Time-resolved difference scattering intensities $q\Delta S(q,t)$ as a function of time delay after photolysis of $\text{Ru}_3(\text{CO})_{12}$ in cyclohexane at 260 nm. The black curves correspond to the experimental data and the red curves to the least-squares fits. Comparison of the time course of the concentration changes of intermediates 1 (black), 2 (blue) and 3 (red) during the photoreaction of $\text{Ru}_3(\text{CO})_{12}$, after excitation b) with 260 nm and c) with 390 nm.

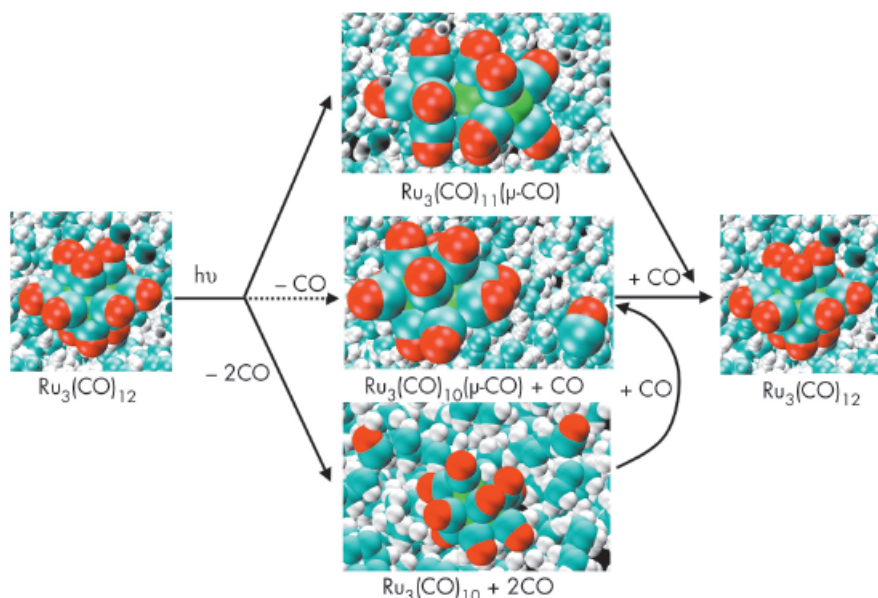


Fig. 71: Ultrafast X-ray solution scattering reveals different reaction pathways in the photolysis of $\text{Ru}_3(\text{CO})_{12}$ at 260 nm and 390 nm. The major difference in the photolysis at 260 nm and 390 nm is due to $\text{Ru}_3(\text{CO})_{10}(\mu\text{-CO})$. After excitation at 260 nm, it is formed from $\text{Ru}_3(\text{CO})_{10}$ by recombination with a free CO, whereas, after excitation at 390 nm, it is formed from the starting molecule $\text{Ru}_3(\text{CO})_{12}$ at the onset of the reaction. The commonality of the reaction between 260 nm and 390 nm excitation is the formation of $\text{Ru}_3(\text{CO})_{10}$ as the major photoproduct. In the figure, the solid arrows show the reaction pathways at 260 nm, while solid plus dash arrows show the reaction pathways at 390 nm.

wavelength absorption band in the UV range has been attributed to metal to ligand charge transfer (MLCT) which ultimately results in loss of one carbonyl group in solution. Ultrafast X-ray solution scattering illustrated that these different absorption processes lead to distinct photofragmentation pathways when $\text{Ru}_3(\text{CO})_{12}$ is excited by different wavelengths. The photodissociation of $\text{Ru}_3(\text{CO})_{12}$ dissolved in cyclohexane was studied on beamline ID09B employing a pump-probe experimental setup. Ultraviolet (260 nm) and visible (390 nm) laser pulses (2 ps) were used for excitation and 100 picosecond X-ray pulses for probing the transient intermediates. In these experiments, the sample flows through a nozzle that produces a layer of liquid of 300 μm thickness. The pump-probe sequence is repeated with different time delays between pump and probe at a frequency of 986.3 Hz and the scattered signal is accumulated on a MarCCD detector. The difference X-ray scattering intensities ($q\Delta S(q,t)$) illustrating the structural changes due to the laser excitation are shown in Figure 70a as a function of different time delays.

Time-resolved X-ray solution scattering on photolysis of $\text{Ru}_3(\text{CO})_{12}$ in cyclohexane at 260 nm and 390 nm reveals different photodissociation pathways. Upon UV excitation at 260 nm, at the onset of the reaction, the species formed are only $\text{Ru}_3(\text{CO})_{11}(\mu\text{-CO})$ for the metal-metal cleavage channel and the intermediate $\text{Ru}_3(\text{CO})_{10}$ with 2 CO loss. In the course of the reaction, the major photoproduct $\text{Ru}_3(\text{CO})_{10}$ then recombines with a free CO to $\text{Ru}_3(\text{CO})_{10}(\mu\text{-CO})$, which eventually decays into the starting molecule $\text{Ru}_3(\text{CO})_{12}$ by recombination with another CO (Figure 70b). After excitation at 390 nm, three intermediates are formed from the initial molecule $\text{Ru}_3(\text{CO})_{12}$ at the onset of the reaction: $\text{Ru}_3(\text{CO})_{11}(\mu\text{-CO})$, $\text{Ru}_3(\text{CO})_{10}(\mu\text{-CO})$ with bridged CO and $\text{Ru}_3(\text{CO})_{10}$ with terminal CO only (Figure 70c). The different photofragmentation pathways of $\text{Ru}_3(\text{CO})_{12}$ in cyclohexane upon UV excitation presumably originate from the higher photon energy which favours the simultaneous loss of two CO leading to $\text{Ru}_3(\text{CO})_{10}$ only for the CO loss reaction channel at the onset of reaction (Figure 71).

References

- [1] T.K. Kim, J.H. Lee, M. Wulff, Q.Y. Kong and H. Ihee, *ChemPhysChem* **10**, 1958-1980 (2009).
- [2] Q.Y. Kong, J.H. Lee, A. Plech, M. Wulff, H. Ihee and M.H.J. Koch, *Angew. Chem., Int. Ed.* **47**, 5550-5553 (2008).

The UV-vis spectrum of $\text{Ru}_3(\text{CO})_{12}$ in cyclohexane has two prominent absorption bands: the first centered at 390 nm and the second with a peak at 238 nm and an absorption shoulder at 260 nm. Electronic absorption studies indicate that the lower energy band at 390 nm originates from the electronic transition $\sigma \rightarrow \sigma^*$ in metal d-orbitals, resulting in heterolytic cleavage of one of the Ru-Ru bonds. The short-